Conference Paper, Published Version

Osorio, Andres; Piedrahita, A.; Arredondo, Maximiliano; Osorio-Cano, Juan; Henao, A.; Cáceres-Euse, Alejandro; Urrego, Ligia; Delgado, Johann

Study of the Velocity and Wave Damping in a Physical Model of a Mangrove Forest Including Secondary Roots

Coastal Structures 2019 - Nils Goseberg, Torsten Schlurmann (eds) - © 2019 Bundesanstalt für Wasserbau
ISBN 978-3-939230-64-9 (Online) - DOI: 10.18451/978-3-939230-64-9_106

Study of the Velocity and Wave Damping in a Physical Model of a Mangrove Forest Including Secondary Roots

A. Osorio, A. Piedrahita, M. Arredondo, J. Osorio-Cano, A. Henao, A. Cáceres-Euse & L. Urrego
Research Group in Oceanography and Coastal Engineering, OCEANICOS, Department of Geosciences and Environment, Universidad Nacional de Colombia, Sede Medellin.

J. Delgado
Coastal Solutions Fellows Program, Cornell Lab of Ornithology, Cornell University, USA and *Research Group in Oceanography and Coastal Engineering, OCEANICOS, Department of Geosciences and Environment, Universidad Nacional de Colombia, Sede Medellin.*

Abstract: The aim of this study was to improve the understanding of flow velocity under oscillatory flow conditions in an artificial *Rhizophora mangle* population (ARmP), in order to promote the use of trees as a natural solution to protect the coasts. The effectiveness of mangrove forests as a wave and velocity-damping structure was studied through physical modeling under laboratory experiments in Universidad Nacional de Colombia – Medellín in a wave-current flume that is able to reproduce linear and 2nd-order stokes waves. Eight wave gauges were implemented along the flume to record the free surface elevation, and a 3-D Acoustic Doppler Velocimeter (ADV; Nortek Vectrino) to measure velocity time series at different vertical positions. The mangrove trees were scaled (1:10) and constructed in stainless steel using a morphometric model to which secondary roots were added. A set of wave scenarios were run for a fixed wave height and several wave periods (H = 0.07 m, T = 1 s - 2 s) and 0.28 m still water level, in order to analyze different non-linearity cases. In most cases, there was a considerable reduction of the steady component velocity inside the ARmP of approximately 30 %, with the velocities increasing with the higher periods. During the experiments, wave damping was 14 % lower than under conditions without mangrove trees. Thus, it can be inferred this structure could be helpful in protecting the coast and reducing erosional processes. Our experiments show the capability of prop roots to reduce the velocity, irrespective of variations in the period, and its capability to reduce wave amplitude.

Keywords: Oscillatory flow, velocities profile, physical model, mangrove forest, primary roots, secondary roots, wave dissipation

1 Introduction

Nowadays, a high percentage of coasts around the world experience erosion, due to the influence of some physical factors, such as sea level rise, extreme wave events and alterations of sediment supply naturally induced or by human actions (Gracia et al., 2018; Linham and Nicholls, 2012). The sea level rise as a consequence of climate change has affected coastal areas, were several biological processes and human activities take place (Linham and Nicholls, 2012). Different strategies of adaptation to climate change have been implemented around the world, especially for coastal protection by hard structures such as retaining walls, dams, spurs, and barriers against storm surge, among others. Soft structure found in coastal ecosystems such as salt marshes, mangroves, coral reefs, seagrasses, crops of halophytic species, among others, give also protect to coasts (McCarthy et al., 2001; Zhu et al., 2010). Many studies on mangroves have demonstrated the efficiency of these ecosystems to protect the coasts from wave actions and, under certain environmental conditions, mangrove also contribute to beach conservation through the sediment retention and rapid inland colonization (Alongi, 2008; Keita Furukawa and Eric Wolanski, 1996; Thampanya et al., 2006; Woodroffe et al., 2016). In addition, mangrove ecosystems provide important ecosystems services, such as refuge for fish and numerous species, water purification and carbon sequestration (Barbier et al., 2011).

The trees of the *Rhizophora* species genus are the most exposed to waves (Feller et al., 2010) among mangroves, and they are also the most tolerant to flooding conditions in coastal ecosystems. These species have an intricate root system responsible for attenuating waves, tides, water currents and sediments (Rodríguez Zúñiga et al., 2013; Tomlinson, 2016). Furukawa and Wolanski (1996) based on field studies, suggested that the amount of roots significantly affects flow velocities, creating eddies, turbulence and influencing the biological processes of mangrove ecosystems. However, there are few studies focused on the hydrodynamics of the flow between tree roots, due in part to difficulties and costs of making field measurements of flow velocities, circulation patterns and sediment transport, influenced by the fact that the majority of mangrove forests are found in countries with few resources (Sato, 2003). These gaps impede the analysis and understanding of the physical processes associated with transport of nutrients and sediments and water currents between the roots of mangroves.

Some authors have modeled the circulation of the water currents within a mangrove under controlled conditions in the laboratory (Maza et al., 2017; Zhang et al., 2015). These authors studied the interaction between long-period waves with the roots as the storm arises, representing the flow as a unidirectional current. To represent the structure of mangrove trees Maza et al. (2017), used a series of parametric equations developed by (Ohira et al., 2013). These authors included in their model only the primary roots of the trees and evaluated the velocities and forces in a model mangrove forest. They found lower speeds of the currents behind the trunks of the trees but higher throughout the roots, avoiding sediment deposition between roots contradicting the hypothesis of sediment retention between mangroves (Keita Furukawa and Eric Wolanski, 1996). Zhang et al., (2015) represented mangrove trees by digital images of the morphology of these trees, considering primary and secondary roots in their physical models. These authors found that aerial roots provided a blocking effect on the flows and caused complex secondary flows. However, these studies do not take into account the interaction between the roots of the trees with the short period waves, located at the edge of the forest, which receive the direct attack of the waves in medium regimes (Mazda and Ikeda, 2006). Studies of water currents and velocities under oscillatory flows have been made in found important relationships between flow velocities and currents with biological processes in these ecosystems (Luhar et al., 2010; Pujol et al., 2013; Zhang et al., 2015). Experiments conducted by Luhar et al., (2010) with physical models of seagrasses recorded a current of considerable magnitude produced in the middle of the canopy of the grasses that was related to the transport of sediments, nutrients and the direction of propagation of the spores and therefore of the colonization of the seagrasses.

To improve the knowledge on the benefits provided by these forests, and to help their inclusion within coastal management plans, it is necessary to increase the understanding of the flow rates between the roots of the forests. The objective of this study is to characterize the wave velocities through the roots of an artificial population of *Rhizophora mangle,* and to evaluate the wave dissipation by this artificial population by of laboratory experiments in a wave channel. To design the physical models that include primary and secondary roots, implementing the methodologies developed by Järvelä, (2004; Ohira et al., (2013) and the field observations of Gill and Tomlinson, (1969). The waves were represented by of oscillatory flows, considering a height of the wave H = 0.07 m, mean water height h = 0.28 m and a systematic variation of the period T (1 s - 2 s). A description of the designed physical model is show in section 2. Section 3 describes the experimental configuration and methods. The results are discuss in section 4, and the most important conclusions are highlight in section 5.

2 Design and scale to model mangrove forest

The intricate system of aerial roots of a mangrove tree is made up of numerous roots in sequential order according to a fractal pattern, ascending from first order to an eighth order (Gill and Tomlinson, 1969; Zhang et al., 2015).

In order to study of the interaction between wave hydrodynamics with the root system, it is important to select a parametric model that closely resembles the structure of a mangrove tree.

For this study, a forest of *Rhizophora mangle* models at scale 1:10 was built, considering the parts of the forest that are most exposed to the flow; these include the trunk and the root system considering only the evaluation of the primary and secondary roots. For the design of the primary roots, we used the methodology provided by Ohira et al. (2013). These authors, through field measurements of 18

trees of the genus *Rhizophora.sp*, developed some allometric equations that allow the formulation of a physical model of the primary root system of these species using only the diameter of the trunk or diameter at breast height (DBH). This methodology for the construction of physical mangrove models has also been implemented by Maza et al. (2017). A DBH = 0.17 m was chosen for the design of the prototype, based on the work from Blanco et al. (2012) for mangroves of mature age present in the Gulf of Urabá, in western Colombia. Using this data in the equations proposed by Ohira et al. (2013), we obtained the dimensions of the prototype shown in Tab. 1 and the physical model shown in Fig. 1.

For the design of secondary roots, we considered the observations made by Gill and Tomlinson (1969) on the morphology of the roots of a mangrove and the methodology of (Järvelä, 2004) used in the mechanical design of trees, which was also used by Zhang, Chua, y Cheong (2015) applied to the design of secondary roots of mangrove trees. The methodology consists of a sequential ordering system of the branches of a tree, and the use of a system of equations to determine the dimensions for each branch. The values obtained for the design of the secondary roots are shown in Tab. 1. The scale was chosen based on the number of Froude and the space available in the channel.

Tab 1. Dimensions of the main parameters of the mangrove prototype

Parameter	Prototype
Diameter at breast height (DBH)	0.17 m
Height of the highest primary root	1.8 m
Horizontal extension of the highest primary root from the trunk	2.94 m
Number of primary roots	19
Average diameter of primary roots	0.032 m
Higher secondary root height	1.47 m
Average diameter of secondary roots	0.026 m
Number of secondary roots	38

The firmness of the roots and trunk of the mangrove models must be rigid enough to represent trees in their natural environment. According to the values of the Young's modulus reported by Zhang et al. (2015) stainless steel rods were used to make the roots and rods of the same material to make the trunks. In order to guarantee the accuracy in the dimensions of the model, templates were created in AutoCAD for the construction of the primary and secondary roots, as well for the location of the roots in the floor. Additionally, marks were made with a nail in the bars, indicating the location of the tie between each primary root and the bars. Finally, all the pieces were joined by welding.

In total, 30 physical models were constructed and distributed in 5 m along the channel in a staggered configuration to produce the overlap of the roots and avoid the formation of preferential flow channels (Fig. 2).

To spread the trees in the channel in a tiered distribution, medium trees located on the walls of the canal were built with the same design used for all the trees. There were 12 medium trees and 18 whole trees in total. The density of the forest was 5.6 arb/m^2 based on the expected density in mature trees with average DBH between 0.11 and 0.20 m, characteristic of the DBH chosen for the model design (Urrego et al., 2014).

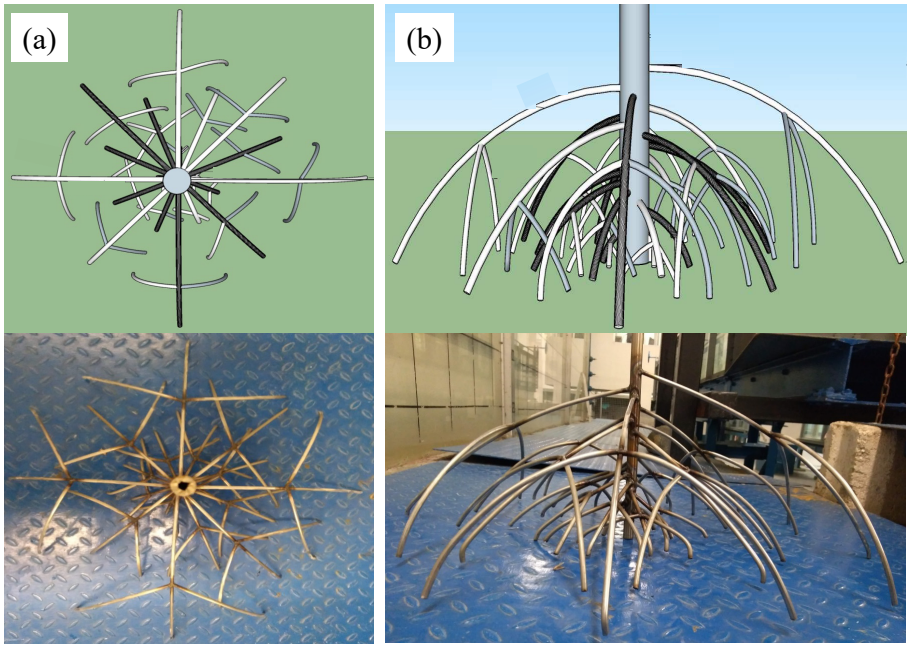

Fig. 1. Physical model of a mangrove tree, (top) design in Google sketchup, (bottom) model built of stainless steel. (a) Top view (b) front view.

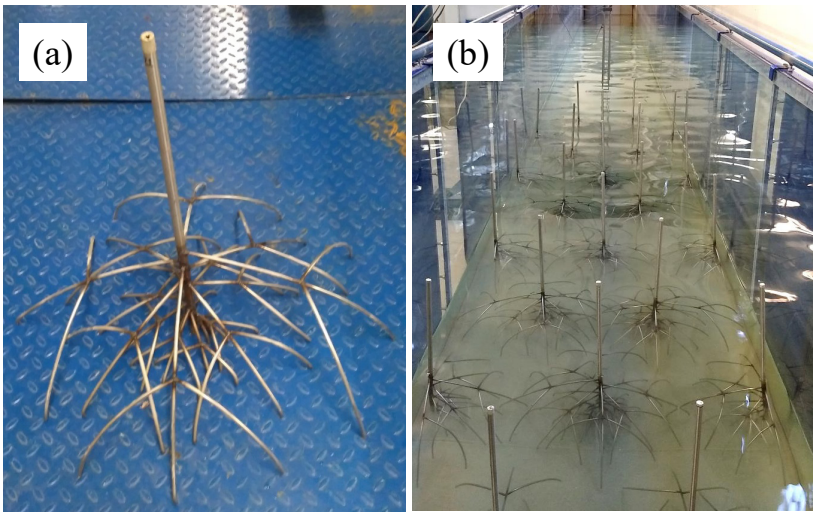

Fig. 2. (a) Mangrove physical model in scale 1:10 (b) stepped arrangement of forests of mangrove models arranged within the channel.

3 Flume experiments

The experiments were conducted at the wave channel of the hydraulic laboratory of the Universidad Nacional de Colombia - Medellín, with dimensions of 25 m long, 1 m wide and 1 m high. The surface waves in the channel is created by a piston-type wavemaker system of the brand HR Wallingford and controlled by a computer software, programmed to produce waves of the desired amplitude and frequency. To dissipate the waves, we installed a beach of nylon foam with a 1:5 slope superimposed on a gravel beach at the opposite end of the channel, producing a reflection percentage between 2% and 20%, depending on the wave parameter. The mangrove forest was located in the middle of the channel to avoid contamination of the wave product of the reflection of the wavemaker and the beach. The experimental setup is shown in Fig. 3.

The velocity profiles were measured using an Acoustic Doppler Velocimeter 3D (ADV, Nortek Vectrino) placed in two different positions. The first one was located at 4.5 m "ADV1" downstream of the wavemaker "x = 0" to measure the velocity incident to the mangrove forest (Fig. 3a). The second location was set at 9.2 m "ADV2" downstream of the wave generation zone to measure the velocities in the fully developed flow zone within the mangrove. Velocities were taken in vertical intervals of 1

cm from z = 2 cm to z = 19 cm, and each point was measured during 6 minutes with a frequency of 50 Hz, registering a total of 180 waves. The ADV2 profile was measured behind a mangrove tree placed between the roots to be able to study the localized effect of the roots on flow velocities. To record the measurement between the roots, we elaborated a mangrove model following the methodology of Ohira et al. (2013), but leaving a space large enough between the roots to introduce the ADV.

Additionally, during the measurement time of the velocities series, wave height were taken by of 8 resistive sensors with fixed carbon-type resistance of the HR Wallingford brand, distributed along the channel, as shown in Fig. 3b. The sensors indirectly measure the elevation of the water with respect to the level of the surface at rest by of the linear relationship between the current and the immersion depth. An amplifier (which supplies voltage to the meters) allows the recording of small voltage changes in a range of 0 to 10 V and then converted into digital time series by a digital analog converter. The sensors have a resolution of ± 0.20 mm in the vertical axis.

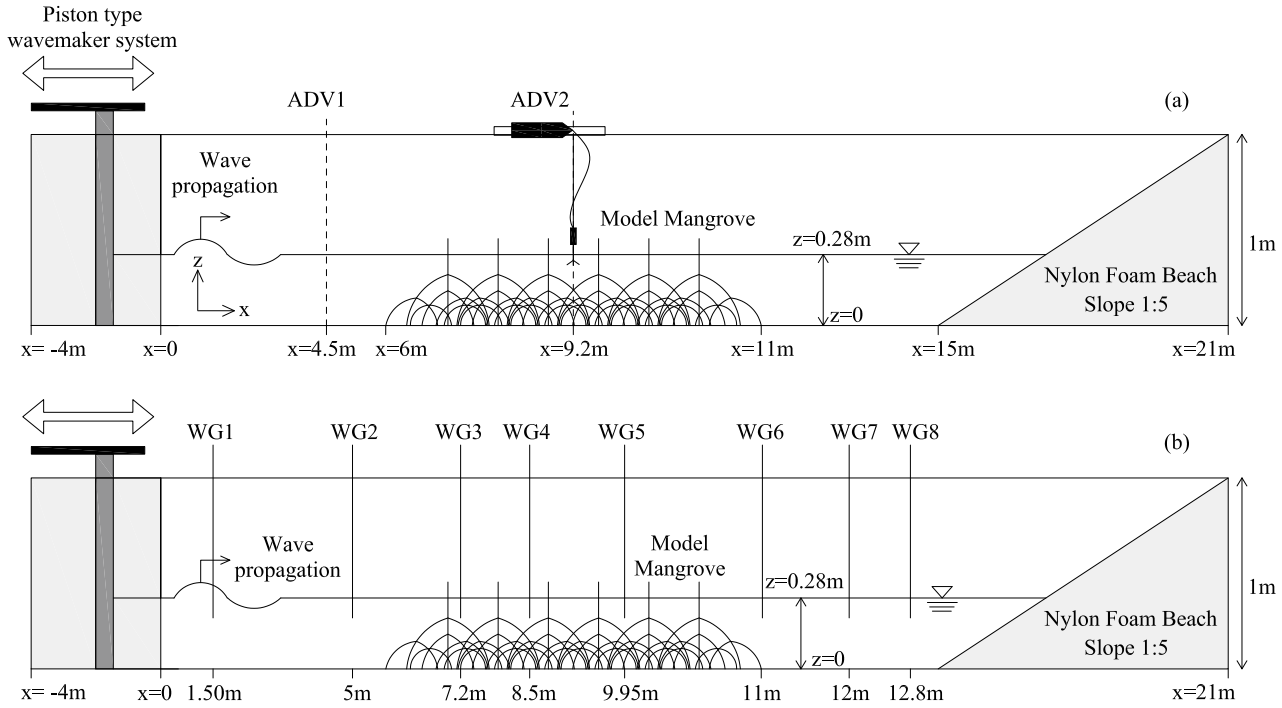

Fig. 3. Experimental setup for (a) velocity measurements, the dashed line indicates measurement locations for vertical profile and (b) wave decay measurement, the solid line represents the wave gauges along the model canopy. Dimensions are in meter but not to scale. The wavemaker and foam beach were located at the upstream and downstream end of the flume, respectively.

For each experimental run, we considered the schematic variation of the period (1 s - 2 s), leaving constant wave height of H = 0.07 m, water depth h = 0.28 m, and forest density. The conditions for each of the tests are shown in Tab. 2.

Tab. 2 Set up for each experiment

Run	h (m)	H (m)	T (s)
T1	0,28	0,07	1
T2	0,28	0,07	1,2
T3	0,28	0,07	1,5
T4	0,28	0,07	1,8
T5	0,28	0,07	2

By of the threshold phase space method proposed by Goring and Nikora (2002), using a code in Matlab, we determined the three components of the velocity obtained with the ADV, and processed by eliminating the noise of the signal and the spikes. In the analysis and results of this article, only the component in the x direction was considered, which corresponds with the highest values of mean

flow. Each instantaneous velocity U_i can be decomposed using the technique of the average phase, according to Eq. (1):

$$U_i = U_c + U_w + u' \tag{1}$$

Where U_c is the steady component velocity, U_w is the oscillatory wave component velocity and u' is the turbulent fluctuation, this technique has been implemented by several authors for the analysis of oscillatory flow in laboratory experiments (Lowe, 2005; Luhar et al., 2010; Pujol et al., 2013; Raupach and Shaw, 1982; Zhang et al., 2018). For the results and analyses of this article, the suffix (c) denotes the steady component velocity, the suffix (w) the oscillatory wave component velocity and the suffix (') the turbulent fluctuation. The component U_c represents the steady component velocity on the x-axis for the set of waves of the entire record and can be calculated by Eq. (2):

$$U_c = \frac{1}{n}\sum_{i=1}^{n} U_i \tag{2}$$

Where n represents the total number of data in the entire record. The oscillatory wave component velocity U_w represents the tangential velocity in an oscillatory flow and is represented by Eq. (3)

$$U_w = \overline{U}_\iota(\varphi) - U_c \tag{3}$$

Where U_i represents the average of all instantaneous velocities in the same phase φ of all waves in the record. $\overline{\varphi}$ is the phase angle of a wave, that is, from $\varphi = 0$ at the beginning of the wave in the zero crossing, $\varphi = 2\pi$ at the end of the wave. U_w is studied by of the root-mean-square (RMS) that gives an idea of its magnitude, in this case being $U_{w,RMS}$ according to Eq. (4).

$$U_{w,RMS} = \sqrt{\frac{1}{2\pi}\int_0^{2\pi}(\overline{U}_\iota(\varphi) - U_c)^2\, d\varphi} \tag{4}$$

4 Result and discussion

The graphs of the velocity profiles of the steady component velocity (U_c) were made at the ADV2 location (Fig. 3) comparing the trials with and without mangrove trees for each of the evaluated periods (Fig. 4). The general effect was the reduction of the speed when mangrove trees were present. As it is shown in Fig. 4, the velocity approach zero in each period, and they reach lower values than the velocity profiles evaluated in the same location under the non-mangrove condition. This result validates the hypothesis proposed by Furukawa and Wolanski, (1996) on the reduction of the speed in measurement on field, produced by the roots of the mangrove trees, which is also consistent with the result obtained by Maza et al. (2017) who reported a reduction in speeds just behind the trunks of the trees for experiment evaluated on unidirectional current. In general, the velocity profiles for different periods showed that for lower periods the slope of the steady component profile is small and negative, and increases as the period increases. As is recorded in Tab. 3 that the lower flow rates are related to low periods and tend to increase as the period increases, this can be observed in the mean values of the components U_c and U_w. The velocities close to zero occurred at a depth between 3 and 5 cm; maximum speeds occurred for depths between 17 and 19 cm. However, in profile T5 the maximum speed occurred at z = 2 cm. High speeds recorded at depths 17 and 19 cm were possibly related to the absence of roots at that depth, and the negative velocities generated inside the channel, that allows the dominance of the return currents as reported by Luhar et al. (2010). When comparing the profiles of the steady component with and without mangrove trees, the greatest difference occurred particularly in periods T1, T2 and T4, where profiles differed by 56%, 71% and 80%, respectively. In addition, the height where the greatest differences occurred seems to indicate that the smaller period the greater effect of the presence of mangrove trees on the profile occurred at approximately 12 cm and the greater effect occurs at 5 cm (Fig. 4).

To compare the runs with and without mangrove trees, graphs of the velocity profiles were made in the RMS oscillatory wave component velocity in location ADV 2 (Fig. 3) for each evaluated period (Fig. 4). As in the steady component, a reduction in the oscillatory component was observe for the non-mangrove tree condition, for each of the periods obtained. The magnitude of this component increased as the period increased (Tab. 3, column 8) and the slope of the profile was positive contrary to the slope of the profile U_c, and increased along with the period. The highest speeds that occurred between 17 and 19 cm were also related to the highest speeds produced by the return currents as recorded by Luhar et al. (2010). For the oscillatory component, it was found that the greatest differences in the mangrove and non-mangrove tree conditions occurred in T3 and T4 and in the depths 7 and 13 cm respectively.

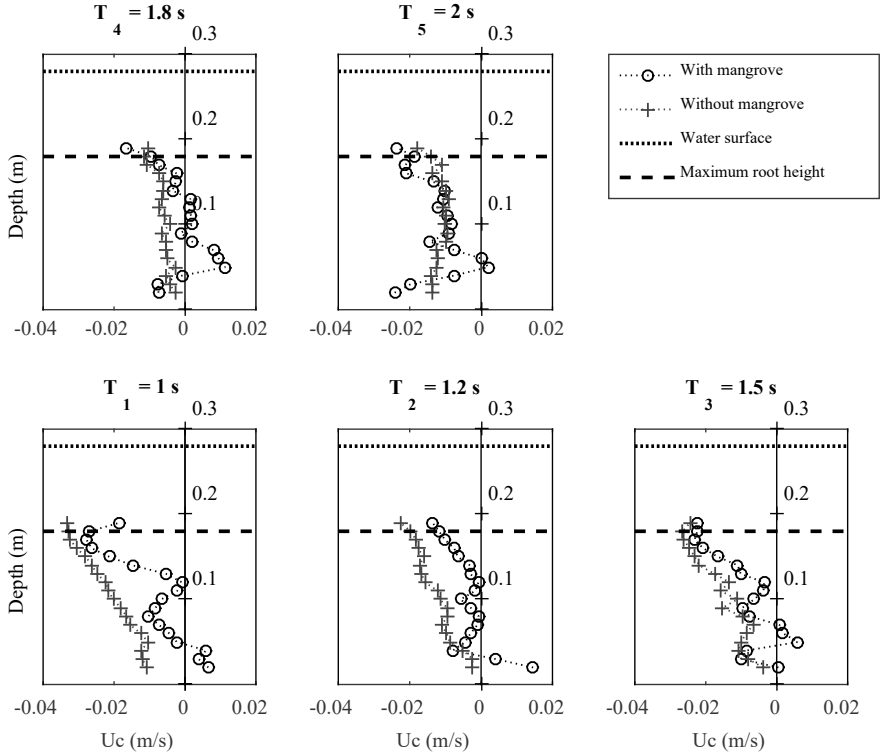

Fig. 4. Vertical profile of the steady component velocity for T (1 s – 2 s), H = 0.07 m y h = 0.28 m.

Based on the free surface series the wave dissipation was analyses for the 5 periods. The greatest dissipation was found for the low periods. As the period increases the dissipation is lower and the increase of the significant wave height over the trees is product of the reflection of the canal, as previously identified by Vanegas et al. (2017) (Fig. 6). As proposed by ASANO, (1988) and Stratigaki et al. (2011) the shorter the period the greater dissipation of wave height.

Tab. 3 Summary of some relevant characteristics found in the velocity profiles obtained in the vertical coordinate z.

Run	T (s)	Uc mean (m/s)	z (Uc=0) (m)	z (Uc=max) (m)	z (Uc*=max) (m)	UcP %	Uw mean (m/s)	z (Uw=max) (m)	z (Uw*=max) (m)	UwP %
T1	1	-0,0093	0,05	0,17	0,12	56,05	0,100	0,19	0,02	4,31
T2	1,2	-0,0036	0,03	0,19	0,12	71,21	0,101	0,19	0,13	2,10
T3	1,5	-0,0093	0,05	0,17	0,11	39,97	0,103	0,17	0,07	10,90
T4	1,8	-0,0012	0,04	0,19	0,05	80,82	0,115	0,17	0,13	6,66
T5	2	-0,0127	0,05	0,02	0,06	6,90	0,124	0,18	0,04	0,95

* Indicates the difference between vertical profile with mangrove and without mangrove (U with M trees. – U without M trees).

P indicates the percentage to difference between the steady component velocity Uc and oscillatory wave component velocity RMS Uw profile with and without mangrove trees.

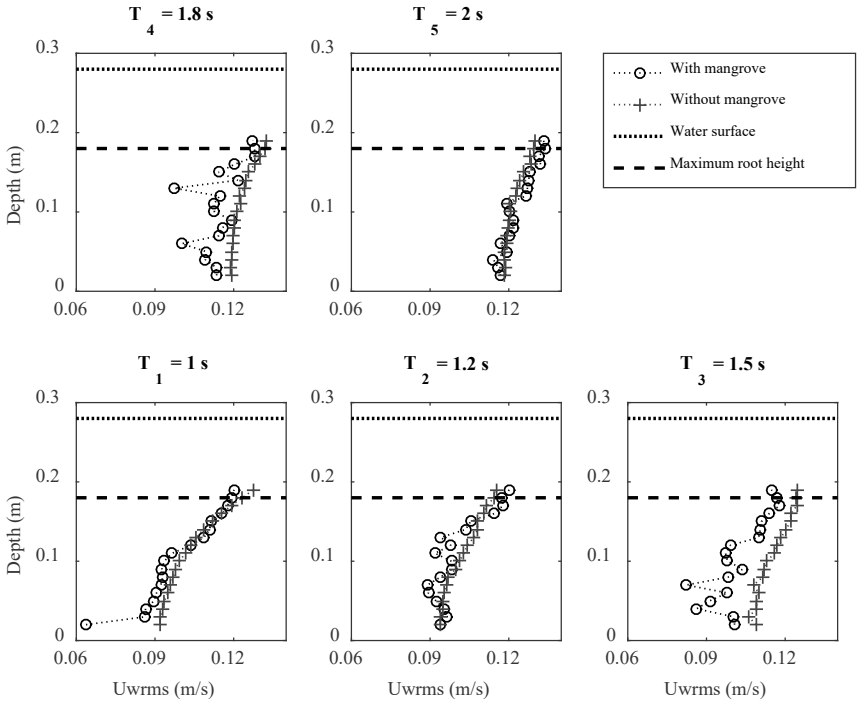

Fig. 5. Vertical profile of RMS oscillatory wave component velocity for T (1 s – 2 s), H = 0.07 m y h = 0.28 m.

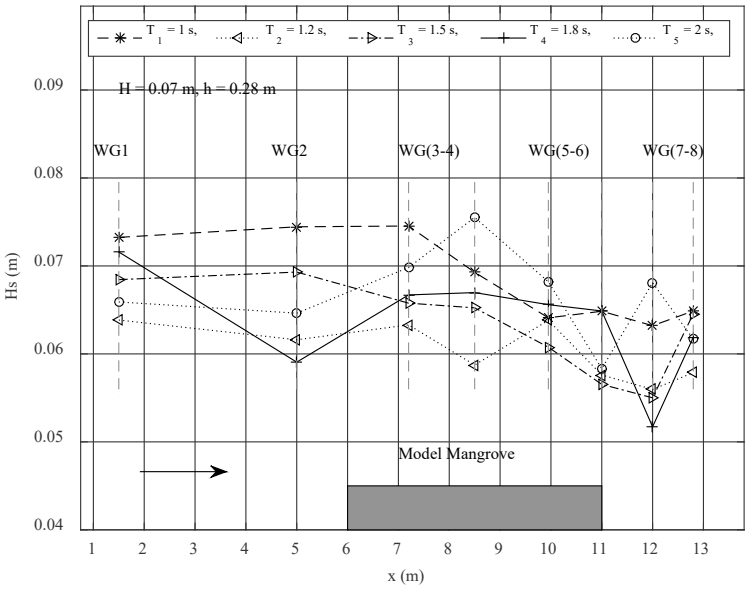

Fig. 6. Wave dissipation on mangrove forest.

5 Conclusions

A model of an artificial population of Rhizophora mangle trees based on the morphology of roots was constructed inside a laboratory channel, following the methodology of Ohira et al. (2013) at 1:10 scale. Velocity and free surface data were evaluated before and inside of the (ARmP), evaluating the condition with and without mangrove trees. A reduction of the speeds was probably related to the measuring point (behind the trunk), where the steady component velocity was of the order of 0.1 m/s at the scale of the model, which at real scale is of the order 0.3 m/s. The increase in the magnitude of the velocities and of the slope of velocity profiles was proportional to the increase in the period, and the higher speeds occurred close to the surface, identified in the steady component as negative velocities close to the surface. These velocities were attributed to the characteristic return current in

the channel. For the steady component velocity, the lowest velocities observed at the position z = 5 cm were attributed to a greater accumulation of roots at this point, although this fact is necessary to analyze it in more detail. Nevertheless, the values of the steady component velocity should be greater than the values obtained, similar to experiments by Luhar et al. (2010) and Zhang et al. (2018), this behavior could be relationship with the reflection and seiches in the channel.

In the analysis of series of free surface, a greater wave dissipation was observed and related to lower periods. However, change in wave dissipation with period increases was not so evident and there was an increase in the height of the wave over the mangrove trees, this increase in the height of the wave is a product of the reflection in the channel (reflection percentage between 2% and 20%, depending on the wave parameter).

Further research should focus on the evaluation of the wave parameters that most influence the behavior of the velocity profile, and to assess if there is a relationship between the morphology of mangrove tree roots and the velocity profile. This could help to study the existence of currents and turbulence produced by mangrove tree roots, and the ecological implications in mangrove ecosystems, associated to the transport of sediments and nutrients, similar to studies carried out in seagrasses ecosystems.

Acknowledgements

This study received support from the Gobernación de Antioquia under the project "*Research of erosion stabilization in the coastlines of Antioquia*". The authors thank Ballantyne Gómez and Santiago Escobar for helping with the flume experiment and to María Maza, and Professor Mauricio Toro for their helpful discussions.

References

Alongi, D.M., 2008. Mangrove forests: Resilience, protection from tsunamis, and responses to global climate change. Estuar. Coast. Shelf Sci. 76, 1–13. https://doi.org/10.1016/j.ecss.2007.08.024

ASANO, T., 1988. Wave damping characteristics due to seaweed. Proc 35th Conf Coast. Engrg 1988.

Barbier, E.B., Hacker, S.D., Kennedy, C., Koch, E.W., Stier, A.C., Silliman, B.R., 2011. The value of estuarine and coastal ecosystem services. Ecol. Monogr. 81, 169–193. https://doi.org/10.1890/10-1510.1

Blanco, J.F., Estrada, E.A., Ortiz, L.F., Urrego, L.E., 2012. Ecosystem-Wide Impacts of Deforestation in Mangroves: The Urabá Gulf (Colombian Caribbean) Case Study. ISRN Ecol. 2012, 1–14. https://doi.org/10.5402/2012/958709

Duke, N.C., Allen, J.A., 2016. Rhizophoraceae (mangrove family) 18.

Feller, I.C., Lovelock, C.E., Berger, U., McKee, K.L., Joye, S.B., Ball, M.C., 2010. Biocomplexity in Mangrove Ecosystems. Annu. Rev. Mar. Sci. 2, 395–417. https://doi.org/10.1146/annurev.marine.010908.163809

Furukawa, K., Wolanski, E., 1996. Sedimentation in Mangrove Forests. ResearchGate 1, 3–10.

Gill, A.M., Tomlinson, P.B., 1969. Studies on the Growth of Red Mangrove (Rhizophora mangle L.) I. Habit and General Morphology. Biotropica 1, 1. https://doi.org/10.2307/2989744

Goring, D.G., Nikora, V.I., 2002. Despiking Acoustic Doppler Velocimeter Data. J. Hydraul. Eng. 128, 117–126. https://doi.org/10.1061/(ASCE)0733-9429(2002)128:1(117)

Gracia, A., Rangel-Buitrago, N., Oakley, J.A., Williams, A.T., 2018. Use of ecosystems in coastal erosion management. Ocean Coast. Manag. 156, 277–289. https://doi.org/10.1016/j.ocecoaman.2017.07.009

Järvelä, J., 2004. Determination of flow resistance caused by non-submerged woody vegetation. Int. J. River Basin Manag. 2, 61–70. https://doi.org/10.1080/15715124.2004.9635222

Keita Furukawa, Eric Wolanski, 1996. Sedimentation in mangrove forest. Mangroves Salt Marshes 1, 3–10.

Linham, M.M., Nicholls, R.J., 2012. Adaptation technologies for coastal erosion and flooding: a review. Proc. Inst. Civ. Eng. - Marit. Eng. 165, 95–112. https://doi.org/10.1680/maen.2011.29

Lowe, R.J., 2005. Oscillatory flow through submerged canopies: 1. Velocity structure. J. Geophys. Res. 110. https://doi.org/10.1029/2004JC002788

Luhar, M., Coutu, S., Infantes, E., Fox, S., Nepf, H., 2010. Wave-induced velocities inside a model seagrass bed. J. Geophys. Res. 115. https://doi.org/10.1029/2010JC006345

Maza, M., Adler, K., Ramos, D., Garcia, A.M., Nepf, H., 2017. Velocity and Drag Evolution From the Leading Edge of a Model Mangrove Forest: VELOCITY AND DRAG IN A MANGROVE FOREST. J. Geophys. Res. Oceans 122, 9144–9159. https://doi.org/10.1002/2017JC012945

Mazda, Y., Ikeda, Y., 2006. Behavior of the groundwater in a riverine-type mangrove forest. Wetl. Ecol. Manag. 14, 477–488. https://doi.org/10.1007/s11273-006-9000-z

McCarthy, J.J., Canziani, O., Leary, N., Dokken, D., White, K. (Eds.), 2001. Climate change 2001: impacts, adaptation, and vulnerability, Cambridge. ed. Cambridge University Press, Cambridge, UK ; New York.

Ohira, W., Honda, K., Nagai, M., Ratanasuwan, A., 2013. Mangrove stilt root morphology modeling for estimating hydraulic drag in tsunami inundation simulation. Trees 27, 141–148. https://doi.org/10.1007/s00468-012-0782-8
Pujol, D., Serra, T., Colomer, J., Casamitjana, X., 2013. Flow structure in canopy models dominated by progressive waves. J. Hydrol. 486, 281–292. https://doi.org/10.1016/j.jhydrol.2013.01.024
Raupach, M.R., Shaw, R.H., 1982. Averaging procedures for flow within vegetation canopies. Bound.-Layer Meteorol. 22, 79–90. https://doi.org/10.1007/BF00128057
Rodríguez Zúñiga, M.T., Acosta Velázquez, J., Carlos Galindo Leal, Cerdeira Estrada, S., Cruz López, M.I., Díaz Gallegos, J., Galindo Leal, C., Jiménez Rosenberg, R., Márquez Mendoza, J.D., Ressl, R., Troche Souza, C., Uribe Martínez, A., Valderrama Landeros, Luis., Vázquez Balderas, B., Vázquez Lule, A.D., Velázquez Salazar, S., 2013. Manglares de México : extensión, distribución y monitoreo. Comisión Nacional para el Conocimiento y Uso de la Biodiversidad (CONABIO), México. https://doi.org/10.5962/bhl.title.111178
Sato, K., 2003. Reality of sedimentation in mangrove forest by the tide and discharge – investigation on trapped amount of deposit in a serial of high tides. A summary on the Mangrove Study in Okinawa. Res. Inst. Subtrop. 58–59.
Stratigaki, V., Manca, E., Prinos, P., Losada, I.J., Lara, J.L., Sclavo, M., Amos, C.L., Cáceres, I., Sánchez-Arcilla, A., 2011. Large-scale experiments on wave propagation over Posidonia oceanica. J. Hydraul. Res. 49, 31–43. https://doi.org/10.1080/00221686.2011.583388
Thampanya, U., Vermaat, J.E., Sinsakul, S., Panapitukkul, N., 2006. Coastal erosion and mangrove progradation of Southern Thailand. Estuar. Coast. Shelf Sci. 68, 75–85. https://doi.org/10.1016/j.ecss.2006.01.011
Tomlinson, P.B., 2016. The Botany of Mangroves by P. Barry Tomlinson [WWW Document]. Camb. Core. https://doi.org/10.1017/CBO9781139946575
Urrego, L.E., Molina, E.C., Suárez, J.A., 2014. Environmental and anthropogenic influences on the distribution, structure, and floristic composition of mangrove forests of the Gulf of Urabá (Colombian Caribbean). Aquat. Bot. 114, 42–49. https://doi.org/10.1016/j.aquabot.2013.12.006
Urrego, L.E., Polanía, J., Buitrago, M.F., Cuartas, L.F., Lema, A., 2009. Distribution of mangroves along environmental gradients on San Andrés Island (Colombian Caribbean). Bull. Mar. Sci. 85, 18.
Vanegas, C., Osorio, A., Urrego, L., 2017. Wave dissipation across a Rhizophora mangrove patch on a Colombian Caribbean Island: An experimental approach. Ecol. Eng. 1–11.
Woodroffe, C.D., Rogers, K., McKee, K.L., Lovelock, C.E., Mendelssohn, I.A., Saintilan, N., 2016. Mangrove Sedimentation and Response to Relative Sea-Level Rise. Annu. Rev. Mar. Sci. 8, 243–266. https://doi.org/10.1146/annurev-marine-122414-034025
Zhang, X., Chua, V., Cheong, H., 2015. Hydrodynamics in mangrove prop roots and their physical properties. Hydro - Environ. Res. 7, 281–294. https://doi.org/10.1080/10643389.2012.728825
Zhang, Y., Tang, C., Nepf, H., 2018. Turbulent Kinetic Energy in Submerged Model Canopies Under Oscillatory Flow. Water Resour. Res. 54, 1734–1750. https://doi.org/10.1002/2017WR021732
Zhu, X., Linham, M.M., Nicholls, R.J., Technical Univ. of Denmark, R.N.Lab. for S.E., UNEP Risø Centre, 2010. Technologies for climate change adaptation. Coastal erosion and flooding.